Performances analysis of combined rankine and absorption refrigeration cycles for a small size solar power plant

Alain C. Biboum[1], Mabvuto Mwanza[1] and Ahmet Yilancı[2]

[1]Ege University, Graduate School of Natural and Applied Sciences, Solar Energy Science Branch, 35100,Bornova, Izmir, Turkey

[2]Ege University, Solar Energy Institute, 35100, Bornova, Izmir, Turkey

Abstract

The use of Concentrating Solar Power (CSP) systems for combined cooling and power (CCP) is increasing daily across the global. However, due to some land and other limitations various types of solar fields, CSP technology and specially solar trough Collector (STC) configuration which may have effect on overall performance of Solar thermal power plant (STPP) are used. Thus, performance analysis of these configurations is vital in order to identify their performance uncertainties and weakness. This paper studies and analysis the performance of three types of STC configuration used in most experimental and non conmmercial plants, using Matlab software and analytical approach. The results shows that for the same modules number, 5Loops configuration has higher performance with energy efficiency of 32.75%, exergy efficiency of 32.07% and lowest coefficient of performance for cooling of 0.5751, followed by 10-SCAs configuration, and 15-SCAs configuration has the lowest performance with energy efficiency of 26.45%, exergy efficiency of 25.91%, and highest coefficient of performance of cooling (COPc) of 0.7706. This study is important for identifying the performance uncertainties of various STC configurations using indirect stem generation (ISG) and selecting the most optimal configuration for small size plant in order to maximize the utilization of solar energy in CSP systems.

.

Keywords: CSP, Solar Collector Assemblies (SCAs), Configuration, CCP, STC, STPP, COPc, ISG, Loop

1. Introduction

Concentrating Solar Power (CSP) systems require direct normal irradiation to effectively function. In order to concentrate the sunlight, the lenses or mirror are used. At the same time, the tracking systems are used to optimize solar thermal power output. The solar trough Collector (STC) can be considered as the most efficiency CSP technology, according with plant number in the world and total energy thermal and electricity production [1]. In California's Mojave Desert Since the 1980s, more than 350 MW of capacity has been developed by the Solar Electric Generating Station (SEGS) using STC technology [2]. A viable alternative that helps to alleviate the challenges associated with renewable energy is a combined cycle (CC) or Rankine cycle power blocks. Solar combined cycle (SCC), uses concentrating solar thermal (CST) energy as the renewable source. V. Zare and M. Hasanzadeh studied closed Brayton cycle combined with Organic Rakine cycle for solar power tower plants in order to optimize electricity generation, in their study they found the efficiencies of the system to be 23.2% [3]. Spelling et al. studied thermodynamic and economic performance of a combined-cycle, based on open air Brayton and steam Rankine cycle was analyzed , in this study it was concluded that the efficiencies of the system was between 18–24% [4]. Organic Rankine cycle (ORC) is a special kind of Rankine cycle that uses an organic fluid as a working fluid instead of water, which is currently used for combined cycle study. ORC could be used with diffferent kinds of low temperatures coming from various heat sources such as geothermal energy, solar energy, biomass energy and waste heat. Suna et Li [5] provided the organic Rankine cycle heat recovery power plant using R134a as working fluid to evaluate and optimize the plant performance. Sun L. et al. [6] proposed an combined power and cooling system power able to use mid/low temperature from heat source, this system consisted of a combination of Rankine cycle (RC) and absorption refrigeration cycle (ARC). During this study Sun L. et al. used the more import portion of waste heat for power generation uusing ORC as was done by V. Zare and M. Hasanzadeh, whereas another portion of this waste heat was used for cooling generation. Today, in order to increase opportunities offered by

doi:10.18086/swc.2017.29.01 Available at http://proceedings.ises.org

renewable energy sources, significant market for the ORC is ready to make more attracted combination of cooling heat and power (CCHP) using waste heat from soloar thermal power plant (STPP) specially. Organic Rankine cycle technology is a challenge to develop an appropriate CCHP scale to meet both energetic, economic and environmental needs increase [7–8]. This paper focus on SCC power plant configuration and performance analysis, in order to show both energetic and exergetic efficiency values of different configurations. In either case this study integrated ARC analysis using waste water from Power combined cycle (PCC) with objective to decrease heat loses.

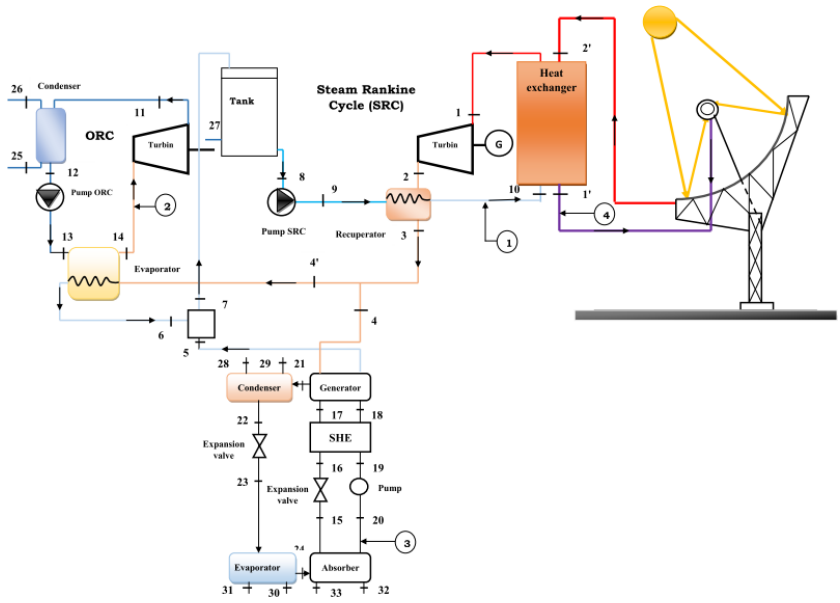

Figure 1: System description

2. System descriptions and assumptions

The following assumptions have been considered in the study

- The system is operating in steady state conditions.
- The kinetic and potential energies and exergies are negleable, due to absence of chemical reactions in the considered system and also in heat transfer fluid.

2.1 System descripton

Fig.1 shows layout of CCP system containing parabolic trough collectors (PTC), heat exchanger , thermal heat transfer fluid and combined power systems able to provide waste heat necessary for cooling system, by using ARC. PTC is a known and commercialized technology. In this study, Luz-S2 and PTR schott technologies are used as receiver type and absorber type respectively. This technology is generally used to provide heat around 500°C using heat tranfer fluids (HTFs) depending o configurtion type, Direct steam generating (DSG) or ISG system. In this case study we are using ISG system on by using Therminol VP-1 as thermal HTF. There after, thermal energy is transfered to water in Intermediate Heat Exchanger (IHE). Before going through IHE, cool water have to be heated by recuperator, to increase its temperature.Steam generated has the temperature close to HTF's temperature according to mass flow rate of water. As indicated in Fig.1 exiting steam from turbine is used for preheating water from tank by using recuperator. Exiting steam from recuperator is used to provide heat for auxilaries cycles both Organic Rankine and Absorption refrigeration. For ORC exiting hot water go through evaporator directly to increase organic heat tranfser fluids temperature (satured vapor state) and for absorption system the hot water is used to seperate Lithium Bromide and Water inside of generator.

2.2 Solar field

Solar energy is one of main key alternative energy sources in Turkey. Therefore, it improtant to consider its utilization in future energy generation mix in the country and especially in Izmir.
Izmir has a mediterranean climate which is characterized by long hot and dry summer with mild to cool and rainy winters[9]. The total average of precipitation for Izmir is around 686 mm per year. However, 77% of the rain falls during December through to March. The maximum temperature during winter months are usually between 10 to 16°C. During summer the ambient air temperature can rise high to as much as 40°C from June to

September. Average relative humidity is between 42 and 70%. Mean monthly sunshine hours are between 124.0 hours in december and 375.1hours in July [9]. Solar energy potential of Izmir is considerable and advantageous due to its geographical position in northern hemisphere as shown in Table 1 [10-11].
During this study direct normal irradation value used for calculation is 523.7 W/m^2, which correspond to Average value of solar radiation during 1 year in Izmir.The solar field can be defined as a system containing a number of loops, with each Loop consisting of two solar collector assembly which is made of connected modules. The specifications of module and Solar Collectors Assemblies is shown in Table 2.

3. Method and Formula

3.1 Configuration Description

Usually there are two arrangement types in Solar thermal collector plant using parabolic trough collectors, I and H. In this study, three differents configurations of STC fied have been analyzed using a same modules number and characteristics. The main aim of this work is to show which configurations can provide better energetic and exergetic efficiencies using CCP system. The configuration type-A contains 15 SCA's and each one has 8 modules without any loop. Configuration type-B contains10 SCA's each with 12 modules without any loop. Configuration type-C contains 5 loops with each one having 24 modules.

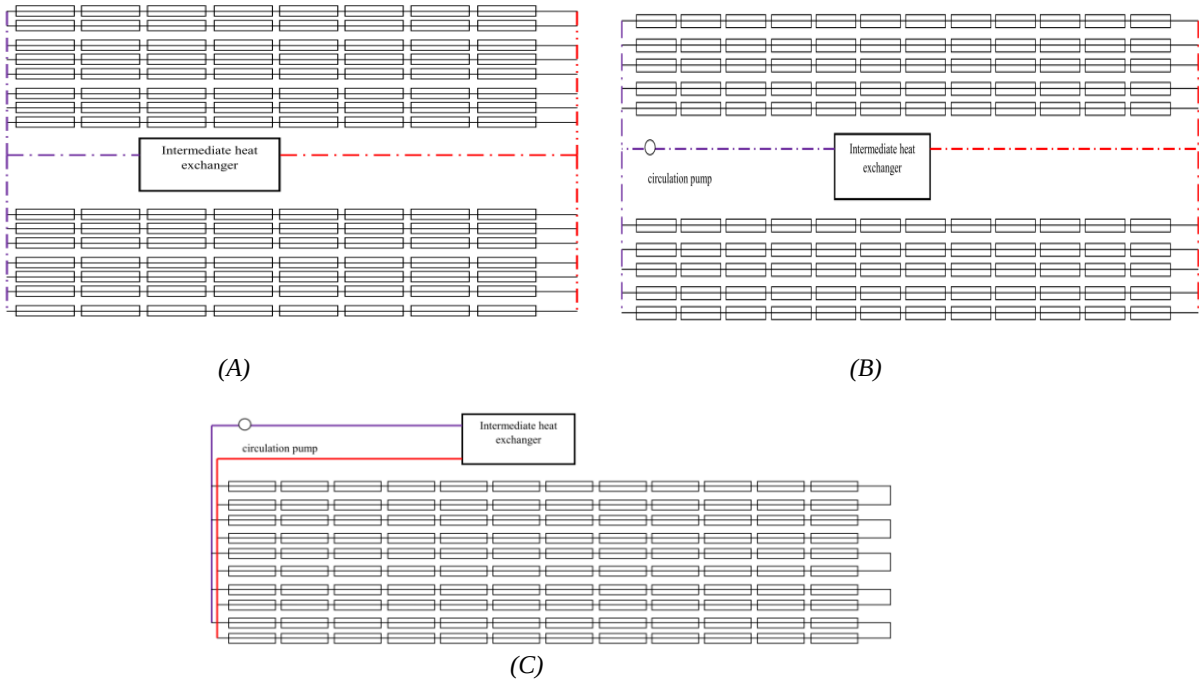

(A) *(B)*

(C)

Figure 2: solar field configurations A, B and C

3.2 Solare collector efficiency

The thermal efficiency of solar collector is the ratio of collector thermal power output to the solar power input [13-15] and can be expressed by eq.1:

$$\eta_c = \frac{\dot{Q}_{abs}}{\dot{Q}_{solar}} \qquad \text{(eq. 1)}$$

Where $\dot{Q}_{solar}$ is the solar power input (kW) and $\dot{Q}_{abs}$ is useful energy output of collector(kW). The solar power input can be calculated from the average direct normal irration G_b and total collector aperture area A_{ap} . Thus, the total available solar on the PTC's cover glass has been estimated using the given eq. 2[15]:

$$\dot{Q}_{Solar} = A_{ap}.G_b \qquad \text{(eq. 2)}$$

The amount of total solar radiation that is striking the collector and used as input heat, which is necessary to heat transfer fluid inside of absorber has been calculated using eq. 3[15].

$$\dot{Q}_{use,in} = A_{ap}.F_R.S \qquad \text{(eq. 3)}$$

Where $\dot{Q}_{use,in}$ is the absorber input solar energy, F_R. is heat removal factor, and S is the heat absorbed by receiver. These parameters can be expressed respectively as[15]:

$$A_{ap} = \left(W - D_{r,o}\right).L \qquad \text{(eq. 4)}$$

$$F_R = \frac{\dot{m}.C_P}{A_r.U_L}\left[1 - exp\left(-\frac{A_r.U_o}{\dot{m}.C_P}\right)\right] \qquad \text{(eq. 5)}$$

$$S = G_b.\eta_o \qquad \text{(eq. 6)}$$

Where η_o is optical efficiency, $U_o$is overall heat transfer coefficient, and $\dot{m}$ is mass flow rate of HTF. The values of a receiver and cover surface area, optical parameters and other can be found in Table 2.
The useful energy output of collector has been estimated using eq. 7 written as[15]:

$$\dot{Q}_{abs} = A_{ap}.F_r.\left(S - \frac{A_r}{A_{ap}}U_L.(T_{ri} - T_o)\right) \qquad \text{(eq. 7)}$$

Where receiver area aperture is A_r (Table), U_L is heat losses coefficience, T_{ri} is input temperature of HTF inside receiver, T_o ambient air temperature. Table 3 summarizes the defination of the optimal parameters of the parabolic trough collector.

3.3 Optical and Thermal analysis of parabolic collector

Therminol VP-1 oil has been used as HTF in this study due to its good temperature control and heat transfer properties (Table 5) [16]. Generally mass flow rate of the heat transfer fluid per row is between 0.35 and 0.8 kg/s according with solar collector assembly length [17]. In order to determine thermodynamic properties of heat transfer fluid entering the IHE and also working fluid properties entering in the steam turbine of Rankine cycle. All the equations below have to be used to calculate the temperature of receiver's cover and the value of solar heat absorbed by the receiver of parabolic trough collector.

A. Optical analysis

The concentration ratio (C) of parabolic trough collector is calculated by the given eq.8 [18]:

$$C = \frac{A_{ap}}{A_{c,o}} \qquad \text{(eq. 8)}$$

The geometric factor is a ratio of lost area to aperture area which is estimated using the following eq. 9[18]:

$$A_f = \frac{A_L}{A_{ap}} \qquad \text{(eq. 9)}$$

Whereas the lost area has been estimated using the expression eq. 10 [18]:

$A_L = \frac{2}{3}W_a.H_p + fW_a\left[1 + \frac{{W_a}^2}{48f^2}\right]$ Where H_P is height of parabola and f is parabola focal distance

Optical efficiency is defined as ratio of the energy incident on the collector's aperture [18]. It depends on optical properties of materials involved, geometric of collector and other parameters as errors related to the construction collector. The optical efficeiency has been estimated using the expression as given in eq11[18].

$$\eta_o = \rho_c.\tau_g.\alpha_r.\gamma\left[\left(1 - A_f.\tan(\theta)\right)cos(\theta)\right] \qquad \text{(eq. 11)}$$

Parabolic Trough collector (PTC) structure uses a two axis tracking, the main advantage of using the tracking system is that solar collector assembly can collect all available direct solar energy during the day, because incidence angle of solar radiation is always equal to zero.

B. Thermal analysis

Generally, in order to decrease the heat losses, a cover glass tube is employed around receiver . The space between the receicer and the cover glass is evacuated in order to minimize the conventional losses. The heat losses coefficient has been calculated usıng eq. 12 given by [18].

$$U_L = \left(\frac{A_r}{(h_{c,c-a}+h_{r,c-a})*A_{c,o}} + \frac{1}{h_{r,r-c}}\right) \qquad \text{(eq. 12)}$$

The heat transfer coeefficients between receiver and cover glass and between cover glass and ambient temparature of have been estimated using eq.13a and 13b written as[18].

$$h_{r,\ r-c} = \sigma\left(T_g + T_a\right)\left(T_g^2 + T_a^2\right).\left(\frac{1}{\varepsilon_r} + \frac{A_r}{A_g}\left(\frac{1}{\varepsilon_g} - 1\right)\right)^{-1} \qquad \text{(eq. 13a)}$$

$$h_{r,\ c-a} = \varepsilon_g\sigma\left(T_g + T_a\right)\left(T_g^2 + T_a^2\right) \qquad \text{(eq. 13b)}$$

The overall heat transfert coefficient, including external walls of the cover glass has been calculated using the following expression eq.14 [18].

$$U_o = \left(\frac{1}{U_L} + \frac{D_{r,o}}{h_{c,r-c}.D_{r,i}} + \frac{D_{r,o}.ln\left({}^{D_{r,o}}/_{D_{r,i}}\right)}{2k_r}\right) \qquad \text{(eq. 14)}$$

Between receiver and cover glass , cover glass and ambient terms of heat trnasfer coefficient are written as eq. 15a and 15b [18]:

$$h_{c,\ c-a} = \frac{(Nu_{air}.k_{air})}{D_g} \qquad \text{(eq. 15a)}$$

$$h_{c,\ r-c} = \frac{(Nu_r.k_r)}{D_g} \qquad \text{(eq. 15b)}$$

Where Nu is Nusselt number, k is the thermal conductivity and D is the diameter of cross section . The Reynold and Prandt number has been estimated using eq.16 and 17 [18]:

$$Re = \frac{V_f.D_{cross}}{\vartheta_f} \quad \text{(eq. 16)}$$

$$Pr = \frac{\rho.Cp.\vartheta}{k} \quad \text{(eq. 17)}$$

By ignoring the radiation absorbed by the cover glass, T_c has been estimated from this energy balance eq.18 :

$$A_c.\left(h_{c,c-a} + h_{r,c-a}\right).(T_c - T_a) = A_r.h_{r,r-c}(T_r - T_c) \quad \text{(eq. 18)}$$

Temperature of receiver cover has been calculated as follows eq. 19 [18].

$$T_c = \frac{h_{r,rc}.T_{r,a} + \frac{A_c}{A_r}(h_{c,ca} + h_{r,ca})T_o}{h_{r,rc} + \frac{A_c}{A_r}(h_{c,ca} + h_{r,ca})} \quad \text{(eq. 19)}$$

C. Thermal efficeincies

The collector efficiency factor for this study has been calculated using eq.20 given by[15-18].

$$F' = \frac{U_o}{U_L} \quad \text{(eq. 20)}$$

The collector efficiency has been found by dividing energy useful by solar energy input. Therefore, the collector efficiency is estimated using the following eq. 21[18].

$$\eta = F_R\left[\eta_o - U_L\left(\frac{(T_{ri} - T_o)}{G_b C}\right)\right] \quad \text{(eq. 21)}$$

The thermodynamic properties of the heat transfer fluid used in the study is given in the Table 5 (Appendix1). Using the heat transfer fluid the usefull energy output of collector has been determined using eq. 22 [15-18].

$$\dot{Q}_{abs} = \dot{m}_{Th}\left(Cp_{Th,o}.T_{Th,o} - Cp_{Th,i}.T_{Th,i}\right) \quad \text{(eq. 22)}$$

Where $\dot{m}_{Th}$, Cp_{Th} and T_{Th} are the mass flow rate , the specific heat and temperature of Therminol VP-1 going trough PTC's receiver respectively. The subscripts o and i refer to outlet and inlet position of Therminol VP-1 inside of that receiver.

3.4 Thermodynamic analysis

Overall system is divided into three subsystems namely, Solar Collector system, Power cycle (Steam and Organic Rankine Cycle), and Absorption system. For each subsystem, thermodynamic models are developed and the components of each subsystem are studied using MATLAB program to simulate the subsystem models. For a control volume accompanying a steady state process the energy and exergy balance equations [19]. Where $\dot{\psi}_{out}$ and $\dot{\psi}_{int}$ are the total exergy rates entering and exiting to the control volume respectively, while $\dot{\psi}_D$ is the exergy destruction rate within the component as defined in Appendix 1.

A. Solar sub -system

Solar subsystem contain essentially PTC and intermediate heat exchanger using Therminol VP-1 oil as working fluid. On the other hand, it's one of the most important part of this system. Its major purpose is provide heat collected from concentrated sun rays to power cycle by intermediate heat exchanger. The energetic efficiency of solar subsystem is the ratio of heat provided by working fluid inside of intermediate heat exchanger to heat obtained through absorber . It has been calculated using eq.28 written as[3,20]:

$$\eta_{th,S} = \frac{\dot{Q}_{IHE}}{\dot{Q}_{use}} \quad \text{(eq. 28)}$$

The exergetic efficiency of solar sub-system is the ratio of the usefull exergy input to power cycle and exergy of heat obtained through absorber. It has been determined using eq. 29 given below[3-20].

$$\eta_{ex,S} = \frac{\dot{\psi}_{2'} - \dot{\psi}_{1'}}{\dot{Q}_{use}\left(1 - \frac{T_o}{T_{ref,sun}}\right)} \quad \text{(eq. 29)}$$

Where $T_{ref,sun}$ is apparent sun temperature as the equivalent heat source temperature (Tref, sun = 5739 K).

The exergy destruction of solar subsystem is the sum of destroyed exergy in intermediate heat exchanger and solar field. It has been estimated using the eq. 30 presented by[3]:

$$\dot{\psi}_{D,solar\ ss} = \dot{\psi}_{D,abs} + \dot{\psi}_{D,IHE} \quad \text{(eq. 30)}$$

B. Power cycle (Steam and Organic Rankine Cycle)

The following assumptions have been considered in the study of the power cycle**:**

- For turbines and pump in Rankine cycles , isentropic efficiencies are assumed as given in Table.
- The appropriate value of the efficiency for recuperator has been assumed as given in table.
- Pressure drop and losses inside of Rankine cycles are neglegible.

$\dot{\psi}_{2'} - \dot{\psi}_{1'}$ represents the usefull exergy input to the combined rakine cycle. Heat provided to power cycle is generated inside of IHE, it has been estimated using the expression given by eq.31[18].

$$\dot{Q}_{IHE} = \dot{m}_w(h_1 - h_{10}) = \dot{m}_f(h_{1'} - h_{2'}) \quad \text{(eq. 31)}$$

While the net output power work $\dot{W}_{net}$ of the combined Rankine cycle has been calculated using eq. 32[15].

$$\dot{W}_{net} = \left(\dot{W}_T - \dot{W}_{Pump}\right)_{SRC} + \left(\dot{W}_T - \dot{W}_{Pump}\right)_{ORC} \quad \text{(eq.32)}$$

Power generation unit converts thermal solar energy absorbed in imtermediate heat exchanger to the net power generated.Thus, the efficiency for both energetic and exergetic of power cycle have been estimated using the following eqs. 33 and 34 respectively[3, 20]:

$$\eta_{th,cc} = \frac{\dot{W}_{net}}{\dot{Q}_{IHE}} \quad \text{(eq. 33)}$$

$$\eta_{ex,cc} = \frac{\dot{W}_{net}}{\dot{\psi}_{2\prime} - \dot{\psi}_{1\prime}} \quad \text{(eq. 34)}$$

For the considered solar power plant the overall energy and exergy efficiency can be defined as ratio of the net output power to the energy or exergy input due to solar irradiation on parabolic collector field. More clearly, power plants overall can be expressed as product of solar field efficiency and power cycle efficiency.
The overall energetic efficiency of power plant has been calculated using eqs. 28 and 33[3]:

$$\eta_{th,PP} = \frac{\dot{W}_{net}}{\dot{Q}_{IHE}} * \frac{\dot{Q}_{IHE}}{\dot{Q}_{use}} \quad \text{(eq. 35)}$$

While the overall exergetic efficiency of power plant has been estimated using eqs. 29 and 34.

$$\eta_{ex,PP} = \frac{\dot{W}_{net}}{\dot{\psi}_{2\prime} - \dot{\psi}_{1\prime}} * \frac{\dot{\psi}_{2\prime} - \dot{\psi}_{1\prime}}{\dot{Q}_{use}\left(1 - \frac{T_o}{T_{ref,sun}}\right)} \quad \text{(eq. 35)}$$

Where $T_{ref,sun}$ is apparent sun temperature.

C. Absorption system analysis

In order to estimate the size of equipment and optimize single effect Water -Lithium bromide absorber cooler. The following assumptions and input values have been considered.

- Absorption system is operating in steady state and refrigerant is pure water.
- There are no pression variation, except through the flow restrictors and the pump (i.e pump and flow restrictors are considered as isentropic and adiabatic respectively).
- Environmental heat losses are neglegible.
- There are no jacket heat losses, and at points 20,17,22 and 24 there is only saturated state.

The cooling COP of absorption system is defined as the ratio of the heat load inside of evaporator and the heat load inside of generator and has beeen determined using expression 38 [22,23] :

$$COP_C = \frac{\dot{Q}_E}{\dot{Q}_G + \dot{W}_P} \quad \text{(eq. 38)}$$

$$= \frac{\dot{m}_{21}(h_{23} - h_{24})}{\dot{m}_{20}(h_{19} - \dot{h}_{20}) + m_{21}h_{21} + \dot{m}_{17}h_{17} - \dot{m}_{18}h_{18}}$$

Where m is mass flow rate and h is the enthalpy of working fluid at each corresponding state point. The heating COP of absorption system is the ratio of combined heating capacity , obtained through absorber and condenser and heat load provided by an external source, specifically inside of generator calculated using eq.39 [22,23]:

$$COP_H = \frac{\dot{Q}_A + \dot{Q}_C}{\dot{Q}_G + \dot{W}_P} = 1 + COP_C \quad \text{(eq. 39)}$$

The exergetic efficiency of absorption system for cooling is exergetic ratio between chilled water at evaporator and heat source at the generator. Which has been calculated using eq.40 [24,25].

$$\psi_C = \frac{\dot{\psi}_{30} - \dot{\psi}_{31}}{(\dot{\psi}_4 - \dot{\psi}_5) + \dot{W}_P} \quad \text{(eq. 40)}$$

The exergetic efficiency of absorption system for heating is exergetic ratio of combined supply of hot water at absorber and condenser to heat source at the generator. Which can be expressed as given in eq.41 [26,27].

$$\psi_H = \frac{(\dot{\psi}_{29} - \dot{\psi}_{28}) + (\dot{\psi}_{33} - \dot{\psi}_{32})}{(\dot{\psi}_4 - \dot{\psi}_5) + \dot{W}_P} \quad \text{(eq. 41)}$$

The exergy destruction of absorption system is defined as the sum of destroyed exergy in each component and can be calculated using the following eq. 42 [28].

$$\dot{\psi}_{D,abs} = \dot{\psi}_{D,Gen} + \dot{\psi}_{D,Con} + \dot{\psi}_{D,\ Eva} + \dot{\psi}_{D,abs}\ \dot{\psi}_{D,she} + \dot{\psi}_{D,Val} \quad \text{(eq. 42)}$$

Table 1 : Energy and exergy balance

Components	Energy Q (kW)			Exergy destroyed I (kW)		
	#1	#2	#3	#1	#2	#3
Absorber	124.1	84.1	55	5.04	6.87	6.82
Generator	124.7	85	57.7	13.81	12.57	11.02
Condens.	101	64.5	35.4	5.77	2.21	1.51
S. he	33	27.4	12.2	2.8	2.58	1.1
Evaporat.	96.1	61.3	33.2	3.15	3.68	1.87
Total				**30.57**	**27.91**	**22.3**

4. Results and Discussion

4.1 Validation of PTSC assemblies

The SCA study is based on the pysical and optical characteristics of the parabolic collector used for its assembly. But for this study the parabolic collector used is the same for all the configurations, moreover we must know that the arrangement of the collectors is in series even if the size and the shape of the SCA show some differences. This validation of the SCA technology was based essentially on the Removal factor, thermal efficiency and thermal efficiency factor (0.85).

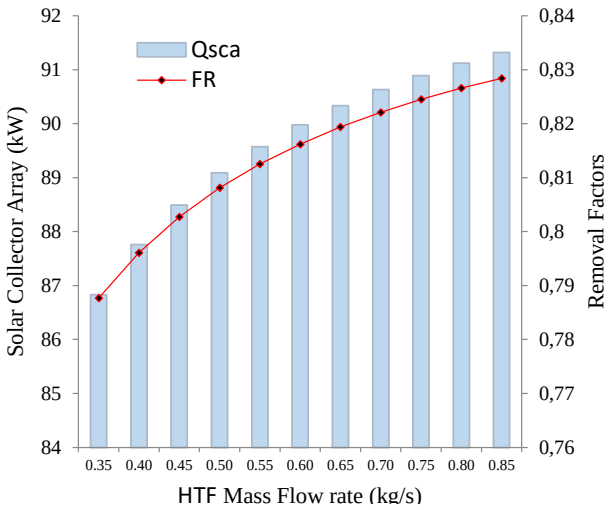

Fig.2: Absorbed energy and Removal factor of SCA. in configuration Type - A

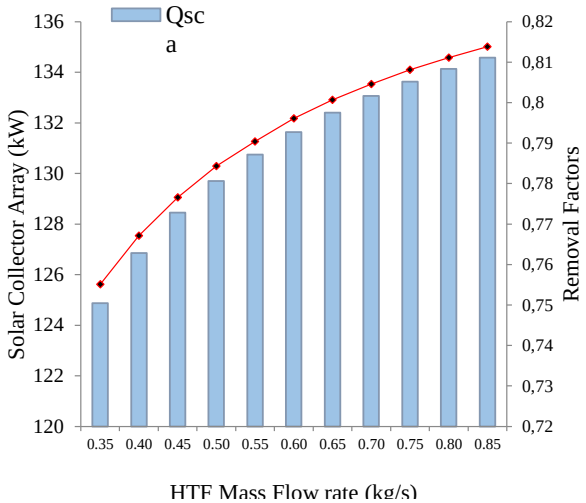

Fig.3: Absorbed energy and Removal factor of SCA. in configuration Type - C

The fig. 2 shows that the SCA used in the configuration type -A has a Removal factor of 0.812 and its energy absorbed of 89.9 kW, while Fig.3 presents a configuration type -B with a Removal factor of 0.791 and an energy absorbed of 131 kW when working with a mass flow rate of 0.55 kg/s. The configuration type-C not shown in this section has a Removal factor of 0.7543 and an energy absorbed of 249.46 kW working at a mass flow rate of 0.65 kg/s.

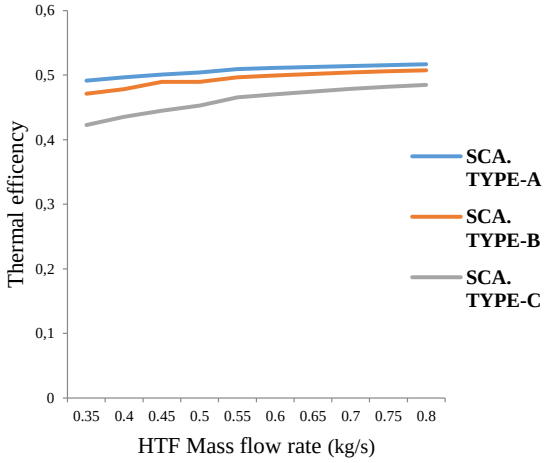

Fig. 4 : Effect of HTF mass flow rate on thermal efficiency.

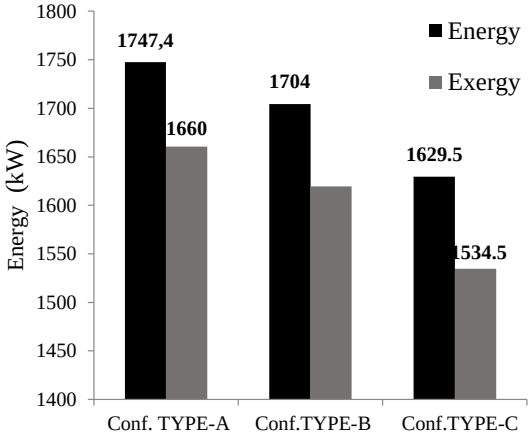

Fig.5: Effects of configuration type on Energy -exergy output

The fig.4 shows a negligible variation of the Thermal efficiency when the mass flow rate increases for the configuration type-A. On the other hand for the configuration type -C there is a considerable variation in the Thermal efficiency when there is a variation of the mass flow rate between 0.35 and 0.7 kg /s. For this study, a mass flow rate of 0.55kg/s will be used for Type-A and Type B configurations and 0.65kg/s for Type-C configuration

4.2 Validation of solar field configuration Type

Fig. 5 shows that the energy absorbed in the configuration type-A is greater than other configurations. It should be noted that the energy absorbed by the configuration of the solar field is closely related to the volume

of transfer fluid used to absorbe that energy. Futhermore outlet temperatures of the transfer fluid in the other types are significantly higher than configuration type-A.
In summary, we will say that the energy absorbed by the solar field changes inversely with the outlet temperature of the transfer fluid. The use of the ORC in the production of electricity does not influence the choice of the appropriate configuration. On the other hand, it contributes to the growth of electricity production in a significant way (Figures 6 and 7).

4.3 effects of configuration on power system performance

A comparative study of the results obtained in Tables 9, 10 and 11 between the CRC and SRC for different configurations shows a relative increase in electricity production according to the type of configuration. The configuration Type -A presents an increase of 5.05%, while configurations type -B and C show 3.1% and 1.95% increase in power generation respectively.

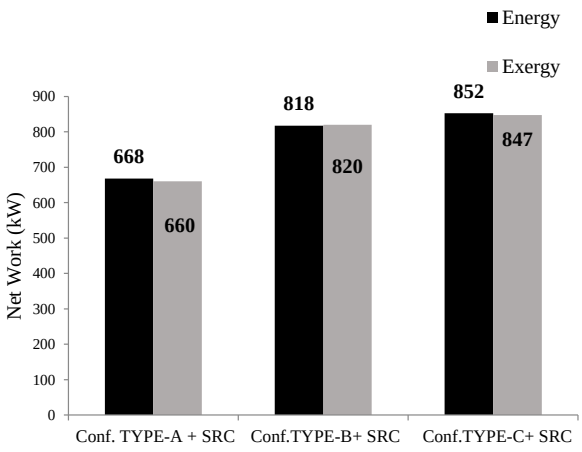

Fig.6: Net work of overall plant without ORC system

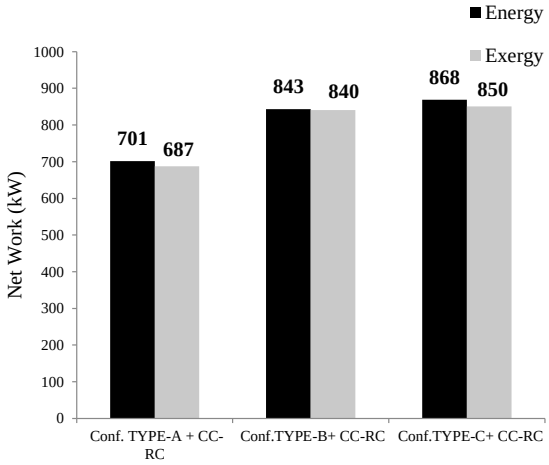

Fig.7: Effect of ORC on power system performance

4.4 effects of additive subsystem on system performance

The figures 8 et 9 show overall performance of studied configurations, configuration Type-C presente an higher performance with energy efficiency of 32.75%, exergy efficiency of 32.07% and lowest coefficient of performance for cooling and heating of 0.5751 and 1.5751 respectively.The configuration Type-C is followed by configuration Type -B, and configuration Type- A. The configuration Type- A has the lowest performance with energy efficiency of 26.45%, exergy efficiency of 25.91%, and highest coefficient of performance of cooling of 0.7706. The fig. 8 presents impact of both ORC and ARC in combined cooling power system analyzed.

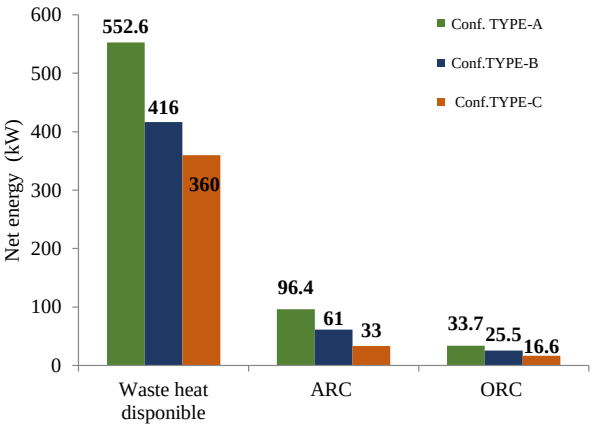

Fig.8: Effect of ARC and ORC on power system performance

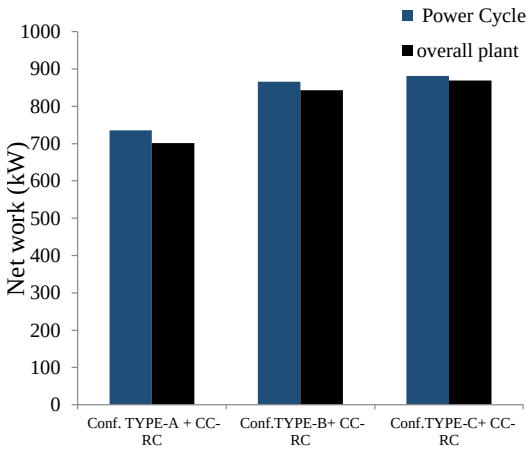

Fig.9: Effect of htf Pumping system on power system performance

Fig. 9 shows direct impact of htf pumping system of solar field configuration type on overall power plant. This study present configuration Type -A as a configuration which transfer 8.25 kg of Therminol oil per second too feed its piping network.

4.5 presentation of other results

Figure 10 presents a complete resume of this study through energy analysis of described system (fig.1). During this study optical, thermal conversion, transport and CCP losses has been analyzed for each solar plant configuration in order to show which of them is more efficiently and can be use to use provide power and cooling more suitably. fig.10.a shows repartition of these losses and overall plant production in configuration Type-A. The total losses evaluated for configuration is 68.62%, where optical losses contribute the highest value of 34.11%, followed by CCP production contributing 26.45% while cooling production contribute the second lowest value of 3.64% and external energy contribute the least lowest value of 1.29%.

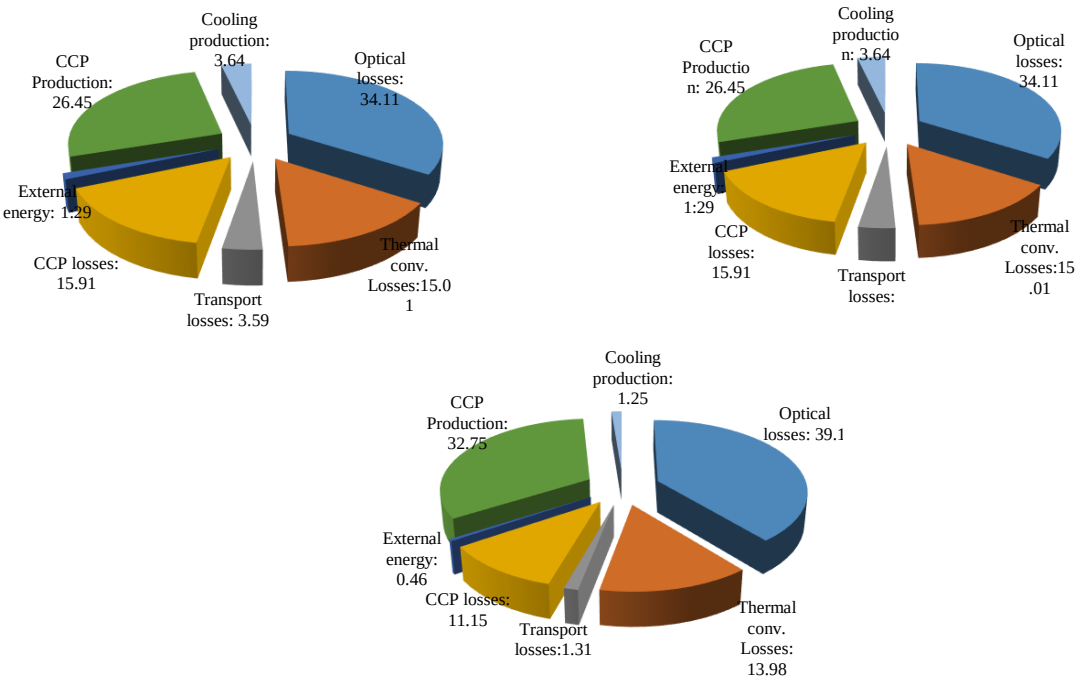

Figure 10: Repartition of energy losses of CCP in plant (a) configuration Type -A (b) configuration Type -B, (c) configuration Type -C

Fig.10.b shows the distribution of the total losses of configuration Type -B with the value of 65.54% , here CCP production contribute 32.75% of the total losses, while cooling production contribute 1.25% and external energy contribute the least value of 0.46%. It is worth to note that in all the configuration, optical losses contribute the highest to losses while external energy contribute the least. Furthermore, among the three configuration studied, configuration type-A had the highest losees followed by configuration type-B, while configuration type-C had the least.

In all the configurations presented, configuration type-C had a higher optical loss and lowest transport, thermal conversion and combined cycles power losses due to higher operating temperature, low mass flow rate of heat transfer fluid and short pipeline network.

5. Conclusion

The complete energy and exergy analysis on combined cooling power using combined Rankine cycles has been analyzed in this paper. This study has considered three differents configuration of same CSP system containing 120 modules. During this study effect of operating parameters such as temperatures, mass flow rates of working, transfer fluids are included, by a situable rate values of each one. Besides this, analysis of individual components of ecah subsystem is also done in order to improve global efficiency of system. This study shown that configuration type-C is more siutable for electricity produce in CSP commercial plant. This configuration despite working with higher temperature and lower mass flow rate, it has higher efficiency for power production. However, the system has lowest absorption refrigeration (AR) system efficiency due to lower exergy transfer by Steam Rankine cycle on the AR system. This study is important for identifying the performance uncertainties of various STC configurations using indirect stem generation (ISG) and selecting the most optimal configuration for small size plant in order to maximize the utilization of solar energy in CSP systems. Thus, its hoped that the results found in this study will be usefull for decision making regarding the selection of CSP systems configurations for optimal solar energy utilization.

References

[1]http://www.nrel.gov/csp/solarpaces/by_country_detail.cfm/country=US%20("_self") [access on23.12.16]
[2] David Ugolini, Justin Z. and John P. 2009. Options for hybrıd solar and Conventional fossil plants, Bechtel Technology Journal.
[3] V. Zare, M. Hasanzadeh 2016. Energy and exergy analysis of a closed Brayton cycle-based combinedcycle for solar power Tower plants, Energy Conversion and Management. 128, 227–237.
[4] Spelling J, Favrat D, Martin A, Augsburger G. 2012. Thermoeconomic optimization ofa combined-cycle solar tower power plant. Energy. 41, 113–20.
[5] J. Suna, W. Li, 2011. Operation optimization of an organic Rankine cycle (ORC) heat recovery power plant, Appl. Therm. Eng. 31, 2032–2041.
[6] Sun L, Han W, Jing X, Zheng D, Jin H. 2013. A power and cooling cogeneration system using mid/low-temperature heat source. Appl Energy.112, 886–897.
[7] M. Imran, B.S. Park, H.J. Kim, D.H. Lee and Al. 2014. Thermo-economic optimization of regenerative organic Rankine cycle for waste heat recovery applications, Energy Convers Manage.87, 107–118.
[8] H. Esen, M. Inalli, M. Esen, 2007. A techno-economic comparison of ground-coupled and air-coupled heat pump system for space cooling, Build. Environ. 42,1955–1965.
[9] https://en.wikipedia.org/wiki/İzmir#Climate [accessed on 15.11.16].
[10] Senol R. An analysis of solar energy and irrigation systems in Turkey. EnergyPolicy 2012;47:478-486.
[11] Topkaya SO, 2012. A discussion on recent developments in Turkey's emerging solar power market. Renew Sustain Energy Rev.16,3754-3765.
[12] https://eosweb.larc.nasa.gov
[13] Janotte, N., Lu¨pfert, E., Pitz-Paal, R., Pottler, K., Eck, M., Zarza, E., Riffelmann, K.-J., 2008. Influence of measurement equipment on the uncertainty of performance data from test loops for concentrating solar collectors. Proceedings of the 14th SolarPACES Conference, Las Vegas, NV (USA).
[14] Kutscher, C., Burkholder, F., Stynes, J.K., 2012. Generation of a parabolic trough collector efficiency curve from separate measurements of outdoor optical efficiency and indoor receiver heat loss. J. Sol. Energy Eng. 134, 11012–11016.
[15] Mohamed S. , Mehmet F. , F. Uygul, 2016.Thermodynamic analysis of parabolic trough and heliostat field solar collectors integrated with a Rankine cycle for cogeneration of electricity and heat, Solar Energy. 136,183–196.
[16] Therminol VP-1, heat transfer fluids by solutia, Applied chemistry, creative solutions, Group Provoc T.B.S 10-04 (12/98) E.
[17] Valenzuela, L., Zarza, E., Berenguel, M., Camacho, E.F., 2005. Control concepts for direct steam generation in parabolic troughs. Sol. Energy. 78, 301–311.
[18] Soteris A. Kalogirou, 2014. Solar Energy Engineering Processes and Systems 2nd edition, ISBN–13: 978-0-12-397270-5
[19] C¸ engel YA, Boles MA.. 1994. Thermodynamics: an engineering approach. New York: McGraw-Hill.
[20] Xu C, Wang Z, Li X, Sun F., 2011. Energy and exergy analysis of solar power tower plants. Appl Therm Eng.31,3904–3913
[21] Talbi MM, Agnew B., 2000. Exergy analysis: an absorption refrigerator using lithium bromide and water as working fluids. Appl Therm Eng.20, 619–630.
[22] Herold KE, Radermacher R, Klein SA., 1996. Absorption chillers and heat pumps. Boca Raton, FL: CRC Press.
[23] Tozer RM, James RW., 1997. Fundamental thermodynamics of ideal absorption cycles. Int J Refrigeration. 20(2), 120–135.
[24] Lee SF, Sherif SA., 2001. Thermodynamic analysis of a lithium bromide/water absorption system for cooling and heating applications. Int J Energy Res. 25,1019–1031.
[26] Talbi MM, Agnew B., 2000. Exergy analysis: an absorption refrigerator using lithium bromide and water as working fluids. Appl Therm Eng.20, 619–30.
[27] Sun DW. Thermodynamic design data and optimum design maps for absorption refrigeration systems.
[28] Kotas TJ., 1985. The exergy method of thermal plant analysis. Great Britain: Anchor Brendon Ltd;
[29] http://re.jrc.ec.europa.eu/pvgis/apps4/pvest.php [accessed on 30.12.16]

Appendix A: Main data and equations

1. Solar Fields and Collector Specification

Table 1: Global solar radiation in izmir [12]

Months	Daily global solar radiation (kW.h/m^2.d.a) [12]	Daily sunshine duration (h/Day) [29]	Av. solar Radiation during Sunshine h. (W/m^2)
January	3.56	9	395.5
February	3.83	9.5	403.2
March	4.99	11	453.6
April	5.33	11.25	473.7
May	6.94	12.75	544.3
June	8.54	11.75	726.8
July	8.83	11.75	751.5
August	8.05	11.75	685.1
September	7.10	11.75	605
October	5.39	11.75	513.3
November	3.75	9.5	394.7
December	2.92	8.75	333.7
Av. values	**5.78**	**11.03**	**523.7**

(source: NASA and JRC)

Table 2: specifications of SCA (SAM Software)

Receiver type	**Luz LS-2**	**Absorber type**	**Schott** PTR80
Reflective area Apperture A_{ap} (m^2)	160.7	Height of receiver in ⊥	4.92
Av. surface to focus path length	1.80	***Absorber tube diameter***	***mm***
Apperture width, W total structure (m)	5	İnner ($D_{r,i}$)	76
Ext. surface areaof Cover glass A_c (m^2)	12.32	Outler ($D_{r,o}$)	80
Ext. surface areaof receiver A_r (m^2)	8.12	***Cover glass . diameter***	***mm***
Length of Module L (m)	8.166	İnner ($D_{g,i}$)	115
Nb modules per collector	-	Outler ($D_{g,o}$)	120
Reflectance mirror (ρ_c)	0.935	İncidence angle modifier (k_r)	1.0
Optical parameters	0.96	***Absorber flow plug***	
Optical efficiency at design	0.87	Internal surface roughness	4.5 e-02
Cover glass Absorbance (α_g)	0.02	Absorber material type	B42 copper
Cover glass Emittance (ε_g)	0.86	receiver absorbance (α)	0.963
Cover glass Transmittance (τ_g)	0.964	Receiver emittance (ε_r)	0.65
Everage heat losses (W/m)	210	İntercept factor (γ)	0.93

Table 3 : Optimal parameters of the parabolic trough collector

Parameter	**Value**	**Symbol**
Useful energy input	-	$\dot{Q}_{use}$
Amount of solar radiation (kWth)	2652	$\dot{Q}_{solar}$
Temperature glass cover (K)	343.5 - 377	T_c
Collector efficiency factor	0.858	F'

2. Heat transfer fluids parameter

$0.1 < Re < 1000$: $Nu_{air} = 0.4 + 0.54.Re^{0.52}$

$1000 < Re < 5.10^4$: $Nu_{air} = 0.3.Re^{0.6}$

$Re < 2300$: $Nu_r = 0.023.(Re)^{0.8}(Pr)^{0.4}$

$Re > 2300$: $Nu_r = 4.364$

Table 5:Properties of thermal Htf and PTC's receiver [16]

Parameter	**Value**	**Symbol**
Therminol / HTF		
Density of HTF @ 15°C	1068 kg/m^3	ρ_{htf}
Thermal conductivity	0.096W/m.K	k_r
Kinematic viscotivity	9.9 10^{-7}m^2/s	υ_{htf}
Thermal conductivity of water	W/m.K	k_{water}
Receiver		
Receiver mass flow rate	> 0.65 kg/s	$\dot{m}_{htf}$
output temprature of receiver	> 665.5K	T_{ro}
input temperature of receiver	503K	T_{ri}
Average solar irradiation	523.7 W/m^2	G_b
Ambient temperature	298.15 K	T_o

3. Thermodynamic of working fluids

Exergy balance equations are expressed in eq.23a, b, and c given below have been used in this study[19]:

$$\dot{E}_{int} - \dot{E}_{out} = \Delta\dot{E}_{syst} \quad \text{(eq. 23a)}$$

$$\dot{\psi}_{int} - \dot{\psi}_{out} - \dot{\psi}_D = \Delta\dot{\psi}_{syst} \quad \text{(eq. 23bc)}$$

$$\dot{S}_{int} - \dot{S}_{out} + \dot{S}_{gen} = \Delta\dot{S}_{syst} \quad \text{(eq. 23c)}$$

For the first law of thermodynamics yields, energy balance of each component is given by eq.23 [19] :

$$\sum(\dot{m}h)_i - \sum(\dot{m}h)_o - \left[\sum Q_i - \sum Q_o\right] + W = 0$$

$$\dot{E} = \dot{m}h \quad \text{(eq. 24)}$$

The exergy of fluid has been estimated using the following expression

$$\psi = (h - h_o) - T_o(s - s_o) \quad \text{(eq. 24)}$$

The exergy destruction in each component has been calculated using :

$$\dot{\psi}_D = \dot{\psi}_{int} - \dot{\psi}_{out} - \left[\sum Q\,(1 - \tfrac{T_o}{T})_i - \sum Q\,(1 - \tfrac{T_o}{T})_o\right] + \sum W$$

$$\dot{\psi} = \dot{m}.\psi \quad \text{(eq. 25)}$$

The exergy destruction of system is the sum of destroyed exergy, can be presented by:

$$\dot{\psi}_{D,Total} = \sum_i \dot{\psi}_{D,i} \quad \text{(eq. 26)}$$

The system performance and optimatization has been done using the presented Thermodynamic law.

The equivalent heat source temperature is given by:

$$\dot{\psi}_{D,CC} = \sum_i \dot{\psi}_{D,T} + \sum_i \dot{\psi}_{D,P} + \dot{\psi}_{D,cond} + \dot{\psi}_{D,Eva} + \dot{\psi}_{D,rec}$$

The governing equations of mass and type of material conservation for a steady state and steady flow system are expressed by eqs. 36a and b[21]:

$$\sum \dot{m}_i - \sum \dot{m}_o = 0 \qquad \text{(eq. 36)}$$
$$\sum(\dot{m}x)_i - \sum(\dot{m}x)_o = 0$$

The heat exchanger efficiency has been estimated using eq. 37 as presented below[18].

$$\pi_{she} = \frac{T_{17}-T_{16}}{T_{17}-T_{19}} \qquad \text{(eq.37)}$$

4. Nomenclature

Table 1: Symbols for Solar Collector and HTF

Quantity	Symbol	Unit
Area Aperture area	A_{ap}	m^2
Area of receiver	$A_{c,o}$	m^2
Lost area	A_L	m^2
Aperture width	W	m
Geometric factor	A_f	
Heat transfer coefficient	h	$W.m^{-2}.K^{-1}$
System mass	m	kg
Concentration ratio	C	
Mass flow rate	$\dot{m}$	$Kg.s^{-1}$
Heat	Q	J
Heat flow rate	$\dot{Q}$	W
Heat flux	q	$W.m^{-2}$
Heat abs. receiver	S	$W.m^{-2}$
Temperature	T	K
Overall heat transfer coefficient	U	$W.m^{-2}.K^{-1}$
Stefan-Boltzmann constant	σ	$W.m^{-2}.K^{-4}$
Removal factor		

Table 2: symbols for materials properties

Quantity	Symbol	Unit
Specific heat	c	$J\ kg^{-1}\ K^{-1}$
Thermal conductivity	k	$W\ m^{-1}\ K^{-1}$
Absorptance	α	
Emittance	ε	
Reflectance	ρ	
Transmittance	τ	
Prandt number	Pr	
Nusselt number	Nu	
Reynold number	Re	

Table 3: symbols for radiation quantities and efficiencies

	Preferred name	Symbol	Unit
a)	Usefull energy output	$\dot{Q}_{abs}$	kWth
	Solar power input	$\dot{Q}_{solar}$	kWth
	Absorbed energy input	$\dot{Q}_{use,in}$	kJ
	Energy	E	kW
	Exergy	ψ	kW
b)	Collector efficiency	η	
	Overall heat transfer	U_o	$W.m^{-2}.K^{-1}$
	Heat losses coefficient	U_L	$W.m^{-2}.K^{-1}$
	Efficiency factor of collector	F'	
	Optical efficiency	η_o	
	Energetic efficiency	η_{th}	
	Exergetic efficiency	η_{ex}	
	Efficiency of exchanger	π	

Table 4 : subscripts

Quantity	Symbol
Glass, Cover glass	*g, c*
destruction	*D*
solar subsystem	*ss*
Absorber, Receiver	*Abs, r*
power plant	*pp*
condenser	*Cond*
evaporator	*Eva*
absorber	*abs*
Thermal	*th*